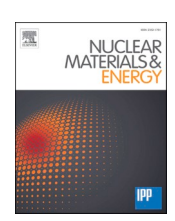
ELSEVIER

Contents lists available at ScienceDirect

# Nuclear Materials and Energy

journal homepage: www.elsevier.com/locate/nme





# Energetic D<sup>+</sup> and He<sup>+</sup> impinging on solid beryllium: Observation of physical and chemically assisted atomic and molecular ion sputtering

Felix Duensing <sup>a</sup>, Faro Hechenberger <sup>a</sup>, Lorenz Ballauf <sup>a</sup>, Anna Maria Reider <sup>a</sup>, Alexander Menzel <sup>b</sup>, Fabio Zappa <sup>a</sup>, Timo Dittmar <sup>c</sup>, Diethard K. Böhme <sup>d</sup>, Paul Scheier <sup>a,\*</sup>

- <sup>a</sup> Institut für Ionenphysik und Angewandte Physik, Universität Innsbruck, Technikerstr. 25, A-6020 Innsbruck, Austria
- <sup>b</sup> Institut für Physikalische Chemie, Universität Innsbruck, Innrain 52c, A-6020 Innsbruck, Austria
- Forschungszentrum Jülich, Institut für Energie- und Klimaforschung Plasmaphysik, Wilhelm-Johnen-Straße, 52425 Jülich, Germany
- <sup>d</sup> Department of Chemistry, York University, Toronto, Ontario M3J 1P3, Canada

#### ABSTRACT

Our Surface-Time-Of-Flight (SurfTOF) tandem mass spectrometer apparatus has been employed in a comparative investigation of ion sputtering induced by monoenergetic  $D^+$  and  $He^+$  ion beams impinging on a Be surface at 700 K with impact energies from 5 to 500 eV. Both chemically assisted sputtering (by  $D^+$  impact below 50 eV) and physical sputtering (by  $He^+$  and  $D^+$  above 50 eV) were observed. Be $^+$  was the dominant sputtered ion at all energies. Chemically assisted sputtering mechanisms are proposed for the concomitant chemical sputtering of  $Be^+$ ,  $Be_2^+$  and  $BeD^+$  ions (by  $D^+$  at low energies). Evidence was also obtained for the sputtering of  $BeO^+$  and  $Be_2O^+$  by both  $He^+$  and  $D^+$  impact ions (with a minimum at 30 eV with  $D^+$ ), but only above 30 eV with  $He^+$ . They are ascribed to the presence of BeO and  $Be_2O$  impurities in the surface layer of Be. Water molecules adsorbed on the Be sample gave rise to  $BeH^+$  and  $BeOH^+$  in the sputtered ion spectrum primarily at higher energies above 30 eV where  $Be^+$  ejection is enhanced. Combined observations with a quartz crystal microbalance and a Faraday cup provided preliminary insight into the sputter yields of neutral and ionized beryllium. These results can be carried over to the erosion of Be by plasma deuterons, and  $T^+$  by extension, in its use as the first wall for the ITER blanket in fusion technology.

#### Introduction

Beryllium has become the first wall material of choice for the ITER blanket directly facing the heat and high-energy neutrons produced during fusion [1-4]. Critical issues in the operation of ITER, among others, are the plasma sputtering erosion of beryllium plasma-facing walls and tritium co-deposition in growing redeposited Be layers. In a fusion device, hydrogen projectiles striking the first wall can enter the wall material and slow down by successive collisions. This can lead to an accumulation of hydrogen in bubbles [5] or the formation of chemical bonds. At higher temperatures diffusion in the material is known [6], whereas chemical binding to beryllium will happen at lower temperatures. These retention processes also influence the blanket stability, but another concern is the inventory of radioactive tritium in the wall materials which has to be limited [7,8]. The problem of tritium retention and the erosion of the wall materials by energetic particle impact including H isotopes and Be has been studied by various experiments and computational modeling [9-20].

Early studies have addressed the erosion of Be as a preferred plasmafacing material [21–24]. More recent studies have focused largely on neutral plasma-induced chemical sputtering of BeD observed experimentally and simulated using molecular dynamics [12,25]. Be samples have been exposed to a deuterium plasma and the erosion of Be atoms and BeD molecules was followed spectroscopically [12,26]. The spectroscopic detection of sputtered ions has been more challenging.

Recently, in our laboratory, we have constructed a new "SurfTOF" tandem mass spectrometer apparatus that allows a Be surface to be exposed to mass-selected projectile ions and for sputtered ions also to be monitored mass spectrometrically [27]. The use of ions allows control of ion energy and the facile detection of sputtered ions. Previous studies in our laboratory with a predecessor of the apparatus used here focused on demonstrating the feasibility of chemically assisted sputtering of Be as  $BeD^+$  using  $D_2^+$  as projectile ions [28].

While  $\mathrm{D_2}^+$  ions are known as impinging species, single atom D or T and single atomic ion D<sup>+</sup> or T<sup>+</sup> projectiles are much more common in ITER technology. We have now successfully generated D<sup>+</sup> projectile ion beams in our SurfTOF apparatus and have been able to perform systematic measurements of the nature of the sputtering of solid Be with D<sup>+</sup>. Furthermore, because we are also able to generate He<sup>+</sup> beams, we also have the opportunity to compare the chemically assisted sputtering that

E-mail addresses: Felix.Duensing@uibk.ac.at (F. Duensing), Paul.Scheier@uibk.ac.at (P. Scheier).

<sup>\*</sup> Corresponding author.

may be induced by  $\mathrm{D}^+$  impact with what must be pure physical sputtering induced by  $\mathrm{He}^+$ .

# **Experimental**

A schematic of the SurfTOF apparatus is shown in Fig. 1; details have been described previously [27]. Deuterium (99.8%, Linde Gas GmbH) or helium gas (99.9999%, Linde Gas GmbH) were introduced with a pressure-controlled gas inlet into an electron impact ion source and ionized at 90 eV. The projectile D+ or He+ ions were selected by a quadrupole (Pfeiffer QMA 400) and impacted on a heated rotatable beryllium surface, 10 mm  $\times$  5 mm (1 mm thick), at 45°. This angle was chosen for practical reasons, and also corresponds to the most probable incident angle with which light ions escaping confinement will interact with the first wall of the fusion plasma [29]. The selected temperature ensures less surface contamination (since adsorbate layers are evaporated) and, above all, is representative of usual temperatures of a reactor wall [1]. A sample holder made from copper is heated ohmically and is equipped with a PT100 temperature sensor between sample and heater, close to the sample. The beryllium sample was supplied by MaTecK GmbH, Germany, with a purity of 99.8% Be. The surface was analyzed with AFM imaging (Azylum Research MFP-3D-Bio) and a roughness of 8 to 10 nm was found across the sample. The surface impact energy was defined by the potential difference between the surface and the ion source. Product ions are collected at 90° with respect to the projectile ion axis and guided to an orthogonal time of flight (TOF) mass spectrometer with a mass resolution (mass/\Delta mass at full width half maximum) of 800. A second pressure-controlled gas inlet for the introduction of surface adsorbates such as water (see "Production of BeH" and BeOH<sup>+</sup>: the influence of surface adsorbed water" section) is placed in front of the surface. For the water measurements the cold-cathode gauge pressure measured in the surface chamber is corrected for water. Differential pumping separates the ion source from the quadrupole and the quadrupole from the surface.

To verify the quantities of the projectile  $D^+$  ions leaving the quadrupole we biased the surface with a reflecting potential to bend the projectile beam into the TOF. The result is shown in Fig. 2.

Measurements were performed at a background pressure of  $2\times 10^{-6}$  Pa. To achieve stable condition, a measurement was started at the earliest after 3 h of sputter cleaning under the same conditions as used for the measurement itself. Depending on the impact energy, the projectile current measured on the surface varied from 0.2 to 0.6nA over an area of 2.2 mm². TOF spectra (12 kHz pulse frequency) were accumulated for 2–6 h, depending on the impact energy.

For the determination of ion yields, the total counts at a certain mass are accumulated and normalized to the projectile  $D^+$  ion current measured on the surface with a 9103 USB picoammeter (RBD Instruments). In the case of He $^+$  no projectile ion current measurement was made due to the high intensity and good long-term stability of this

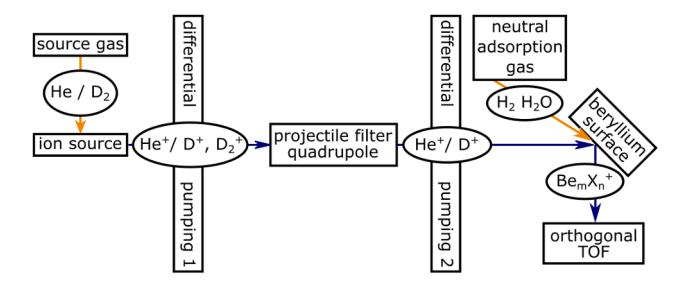


**Fig. 1.** Concept sketch of the experimental apparatus. The source gas  $D_2$  or He is ionized by electron impact in the ion source and the resulting ions are m/z filtered by a quadrupole. Neutral gas can be adsorbed on the surface. Secondary ions leaving the surface sample can be analyzed with an orthogonal pulsing, reflectron time-of-flight mass spectrometer (TOF). The complete setup is described in [27].

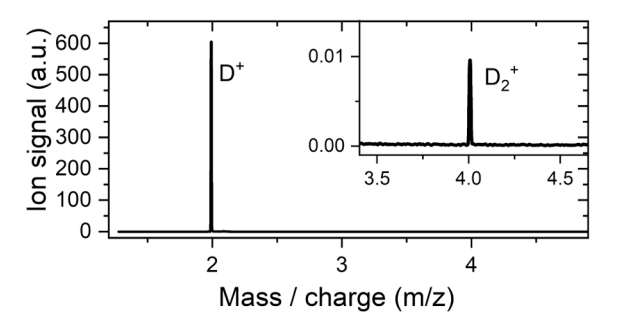


**Fig. 2.** TOF mass spectrum of the projectile  $D^+$  ions. The ions were bent by a reflecting potential of 22 V on the surface. The ratio of  $D^+/D_2^+$  yields was measured to be  $6\times 10^4$ .

ion beam. The TOF measurements show only an unknown fraction of the total ion yield coming from the surface, but it can be assumed that this is similar for all ions.

The elemental composition of the beryllium target surface and the ion optical lenses in the region of the target surface was probed by XPS measurements using a Thermo MultiLab 2000 spectrometer with an alpha 110 hemispherical analyzer (Thermo Electron) in the constant analyzer energy mode (pass energy 100 eV, overall energy resolution 2.2 eV). A twin crystal monochromator provided focused Al K-alpha radiation (1486.6 eV, spot diameter 650 um) [30].

#### Results

The deuterium isotope  $D^+$  was chosen over  $H^+$  as a projectile ion due to its relevance to fusion and to avoid obfuscation that may arise from H-containing impurities that may cover the surface, especially water and possibly hydrocarbons. We wanted to make sure to be able to distinguish between beryllium hydride ions produced from impurities on the surface,  $BeH^+$  produced from  $H_2O$ , and beryllium hydrides produced by the surface, as  $BeD^+$  rather than  $BeH^+$ .  $He^+$  was chosen as a projectile to provide a comparison with sputtering behavior restricted to physical sputtering.

### Mass spectra

The two mass spectra in Fig. 3 show the secondary ions recorded at a high (347 eV) and a low (48 eV) impact energy of the He<sup>+</sup> projectile. Our scans up to m/z 1300 showed no significant ions beyond m/z = 45.

At the lower energy of 48 eV a few minor ions originating from impurities in the Be target as well as the ion optical lens surrounding the

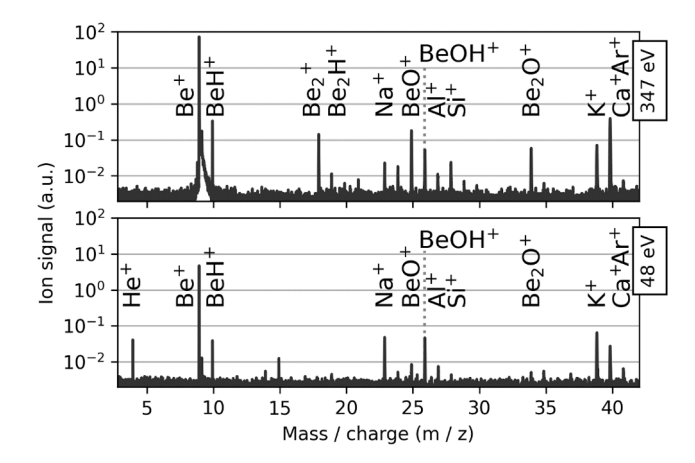


Fig. 3. Two mass spectra for sputtered ions recorded with  ${\rm He^+}$  projectile ions bombarding a heated (700 K) Be surface at 48 eV and 347 eV. Note that the exponential scale for the ion yield spans 4 orders of magnitude.

collision region are present. The sputtered Be-containing ions are dominated by Be<sup>+</sup> and Be<sub>2</sub><sup>+</sup>, their hydrides BeH<sup>+</sup> and Be<sub>2</sub>H<sup>+</sup>, and their oxides, BeO<sup>+</sup> and Be<sub>2</sub>O<sup>+</sup>. All increase at the higher He<sup>+</sup> projectile energy. As do m/z=28 and 40 which we assign to Si<sup>+</sup> and Ca<sup>+</sup> since Si and Ca are impurities in Be known from previously reported TOF-ERDA elemental profiles for Be [28]. The m/z=26 ion is assigned to BeOH<sup>+</sup> according to results obtained in separate experiments with water.

We attribute the origin of the impurity ions Na $^+$  (m/z=23), Al $^+$  (m/z=27) and K $^+$  (m/z=39 and 41) to their sputtering from stainless-steel lenses surrounding the Be sample. Separate experiments, using Ar $^+$  as a projectile, showed that these ions are also sputtered from a stainless-steel sample replacing the Be target. XPS measurements of the stainless-steel show small amounts of Na and K (2.1% and 1.2% respectively) and due to their low ionization energies, they are more present in the mass spectra. Al $^+$  probably originates from milling tools that were used to manufacture aluminium parts before manufacturing the stainless-steel ion optics of this experiment.

The two mass spectra in Fig. 4 show the secondary ions recorded at a high (269 eV) and a low (48 eV) impact energy of the D<sup>+</sup> projectile. Again, our scans up to m/z=1300 showed no significant ions beyond m/z=45.

The primary  $D^+$  projectile ions appear to be completely consumed upon surface impact.  $Be^+$  is by far the most abundant sputtered ion, surpassing most observed secondary ions in intensity by at least two orders of magnitude (the  $K^+$  yield reaches within one order of magnitude at the higher energy of 269 eV). The ions  $Be^+$ ,  $Be_2^+$  and possibly  $Be_3^+$  (isobaric with  $BeOD^+$ ) that can be derived directly by physical sputtering from the Be surface are clearly visible.  $BeO^+$  and  $Be_2O^+$  can also be attributed to surface sputtering since previously reported TOF-ERDA elemental profiles indicated abundant O atoms near the surface of Be (due to the lower projectile flux when using  $D^+$  compared to  $D_2^+$ , the BeO layer does not appear to be removed during the course of the experiments, as it was the case in [28]).

 $\mbox{BeD}^+$  and  $\mbox{BeOD}^+$  are both signature ions of the  $\mbox{D}^+$  projectile in that they contain both deuterium and beryllium.  $\mbox{BeOD}^+$  is very likely a signature ion of the presence of BeO impurity in the pure Be surface as well. XPS measurements have shown that BeO is a trace constituent of the sample Be surface, probably arising from some surface oxidation of the sample while in storage and in transit.

BeH<sup>+</sup> and BeOH<sup>+</sup> (m/z = 26) are likely to arise from the interaction of Be<sup>+</sup> (and perhaps also Be<sub>2</sub><sup>+</sup> and Be<sub>3</sub><sup>+</sup>) and BeO<sup>+</sup> with H<sub>2</sub>O on the Be surface, as has been demonstrated in the previous D<sub>2</sub><sup>+</sup> projectile experiments [28].

The assigned  ${\rm CH_3}^+$  ion likely arises from ambient hydrocarbon impurities. We also observed again the impurity ions  ${\rm Na}^+$  (m/z=23) and

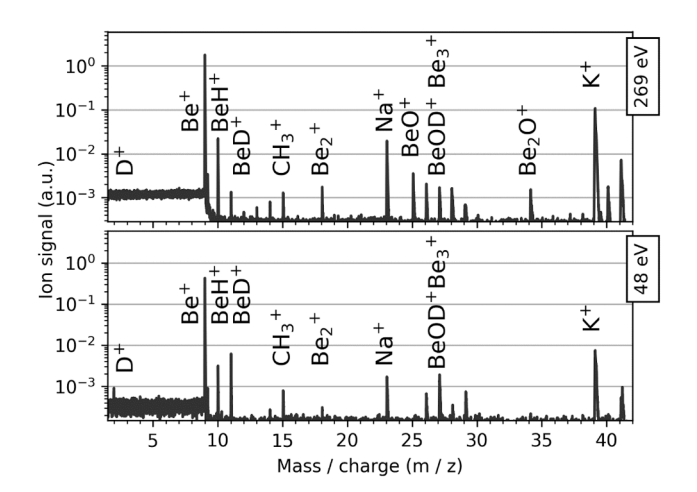


Fig. 4. Two mass spectra for sputtered ions recorded with  $D^+$  projectile ions bombarding a heated (700 K) Be surface at 48 eV and 269 eV. Note that the exponential scale for the ion yield spans 4 orders of magnitude.

 $K^+$  (m/z = 39 and 41), as well as  $Si^+$  at m/z = 28 and  $Ca^+$  at m/z = 40 derived from Si and Ca impurities in the Be as observed in the previously reported TOF-ERDA elemental profiles for Be [28].

Surface impact energy scans with He<sup>+</sup>

The sputtered Be-containing ions Be $^+$  and Be $_2^+$  and their oxides, BeO $^+$  and Be $_2$ O $^+$ , were monitored with increasing surface impact energy of the He $^+$  projectiles at a surface temperature of 700 K. The results are shown in Fig. 5. The ion yield is defined as a detection rate for each mass per charge divided by the incident projectile current. Since the detection efficiency is not known, we use arbitrary units (a.u.) in our graphs. The detection efficiency is expected to be mass independent in the range of the ions of interest.

The Be $^+$  profile shows an immediate onset with a strong rise and is by far the most dominant sputtered ion at surface impact energies above 50 eV (all others are < 1%). The ions BeO $^+$  and Be<sub>2</sub>O $^+$ , likely derived from BeO and Be<sub>2</sub>O impurities in the Be, have similar profiles. The Be<sub>2</sub> $^+$  dimer ion profile shows a distinctly higher onset at around 50 eV (< 0.1% of Be $^+$ ) and a more persistent rise than Be $^+$ .

Surface impact energy scans with  $D^+$ 

Fig. 6 shows that the ion erosion of pure beryllium at 700 K with  $D^+$  projectiles also proceeds largely by the expulsion of atomic  $Be^+$  at all impact energies, dominating all other sputtered ions by more than two orders of magnitude. Noteworthy is the substantial erosion of  $Be^+$  already at 5 eV with an apparent enhancement at around 30 eV.

In comparison to Be $^+$  erosion, only trace amounts of the dimer ion Be $_2$ <sup>+</sup> are eroded, especially above 100 eV. The identity of the signal at m/z=18 at energies below 90 eV is more ambiguous since Be $_2$ <sup>+</sup> is isobaric with H $_2$ O $^+$ . The ion yield in Fig. 4 of m/z=27, Be $_3$ <sup>+</sup>, isobaric with BeOD $^+$  and Al $^+$  (not shown in Fig. 6), had a very low value of  $10^3$ , roughly independent of surface impact energy. The erosion of atomic and molecular beryllium ions conceivably is accompanied by residual D implantation in the Be metal.

The appearance of BeD<sup>+</sup> at low energies and its subsequent profile are particularly noteworthy. BeD<sup>+</sup>, the only deuterium/beryllium containing ion that was observed to be sputtered with D<sup>+</sup> as the projectile ion can be regarded as a signature ion for the chemically assisted sputtering of Be in the sense that the sputtering of BeD<sup>+</sup> involves Be-D chemical bond formation. The BeD<sup>+</sup> yield shows a maximum at 50 eV, close to the onset in the high energy Be<sup>+</sup> (D<sup>+</sup>) profile but then decreasing continuously with increasing D<sup>+</sup> impact energy while the Be<sup>+</sup> signal remains high. BeD<sup>+</sup> sputtering also was observed in our earlier studies with D<sub>2</sub><sup>+</sup> projectile ions [28], Fig. 6 shows a distinctly different response

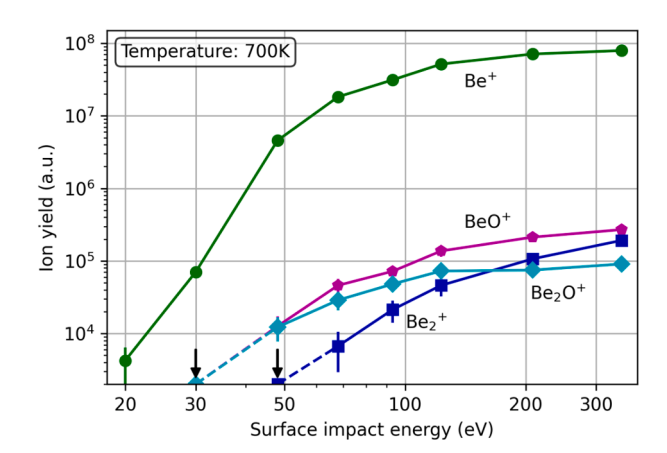


**Fig. 5.** Product ion yields in response to the surface impact energy (laboratory-frame) of  ${\rm He^+}$  on Be at a surface temperature of 700 K. Data points designated with an arrow are below the noise level.

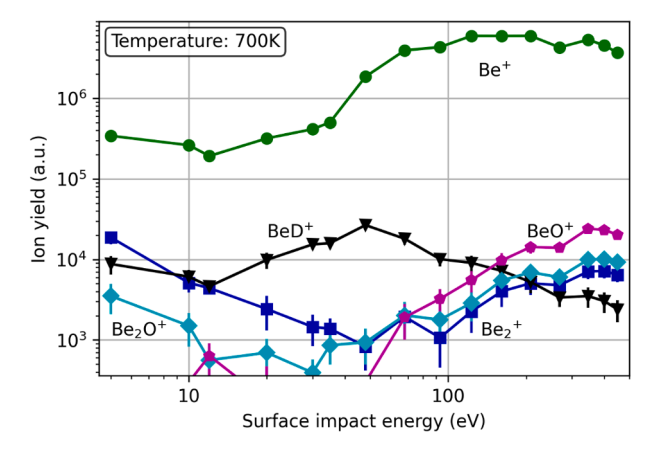


**Fig. 6.** Product ion yields in response to the surface impact energy (laboratory-frame) at a surface temperature of 700 K. Yields are the number of sputtered ions in arbitrary units divided by the projectile  $D^+$  ion current.

of sputtered  $BeD^+$  to the  $D^+$  surface impact energy than either  $Be^+$  or  $Be_2^+$ . Its ion yield profile is quite unique: the appearance onset is lower and much more gradual and the yield peaks at 50 eV, at which it is the second most abundant sputtered ion, before diminishing to low values at higher  $D^+$  impact energies.

Comparison of surface impact energy scans with  $He^+$  and  $D^+$ : physical vs. chemical sputtering

Fig. 7 provides a direct comparison of the surface impact energy scans obtained with He $^+$  and D $^+$  impact ions for the sputtering of Be $^+$ , BeD $^+$  and Be $_2$  $^+$ . There are striking differences in the measured profiles for He $^+$  and D $^+$  at low energies and similarities at high energies. At low impact energies, < 20 eV, Be $^+$  and Be $_2$  $^+$  are not sputtered by He $^+$  projectiles but at higher energies, > 50 eV, the profile shapes for sputtered Be $^+$  and Be $_2$  $^+$  tend to converge for the two projectile ions.

The low-energy anomaly of the sputtering of Be $^+$  and Be $_2^+$  (and BeD $^+$ ) only with D $^+$  projectiles must be attributed to the occurrence of chemically assisted sputtering. A mechanistic interpretation of this sputtering needs to also take into account the theoretical predictions of the occurrence of highly-probable neutralization of the D $^+$  projectiles by electron transfer just before surface impact [31–33]. We can envisage bond formation at impact with the resulting deuterium radicals to form BeD upon encountering and entering the Be surface. Be-D bond formation at the surface is expected to lower the surface binding energy in the

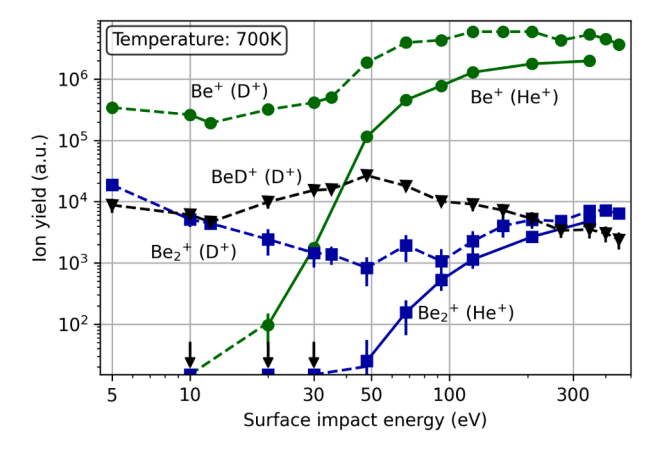


**Fig. 7.** Product ion yields in response to the surface impact energy (laboratory-frame) at a surface temperature of 700 K.  $(D^+)$  yields are normalized to the projectile  $D^+$  ion current,  $(He^+)$  yields are scaled to be visible in the same range. Data points designated with an arrow are below the noise level.

metal and possibly eject BeD by a second incoming projectile. Indeed, previous deuterium plasma impact experiments with Be have demonstrated the sputtering of neutral BeD at low energies [12]. Under our conditions, subsequent  $D^+$  impact of an emerging BeD molecule can lead to  $Be^+$ , as well as  $BeD^+$  formation according to reaction (1):

$$D^{+} + BeD \longrightarrow Be^{+} + D_{2}$$
 (1a)

$$D^{+} + BeD \longrightarrow BeD^{+} + D \tag{1b}$$

Both channels likely are energetically favorable. It is noteworthy in this regard that according to [12]  $D_2$  molecules were not seen to be sputtered in the deuterium plasma impact experiments but in MD simulations they were. Reaction (1) would account for the low-energy formation of Be<sup>+</sup> and BeD<sup>+</sup>. An analogous mechanism could account for the low-energy formation of Be<sub>2</sub><sup>+</sup> from reaction (2) if the deuterium radical inserts into a Be-Be bond in the metal and releases Be<sub>2</sub>D:

$$D^+ + Be_2D \longrightarrow Be_2^+ + D_2 \tag{2}$$

If neutralization of  $D^+$  prior to impact is incomplete, formation of  $Be^+$ ,  $BeD^+$  and  $Be_2^+$  could proceed more directly with the (un-neutralized)  $D^+$  impacting and penetrating the Be surface.

As regards the observed trends with energy at low energy, we note from the reported D plasma impact experiments the decay in the fraction of Be sputtered as BeD from 10 to 100 eV [12]. This is consistent with the decrease observed in our experiments for the fraction of Be sputtered as  $BeD^+$  with increasing ion energy up to 93 eV.

The mechanism leading to the peak in the profile for  $BeD^+$  at 50 eV and the subsequent decrease in  $BeD^+$  at higher energies is less certain. Perhaps there is less neutralization of  $D^+$  to form D and subsequently BeD, or a decrease in the efficiency of electron transfer from BeD to  $D^+$  at the higher energies.

With  ${\rm He}^+$  impact ions, the onsets for the production of  ${\rm Be}^+$  at 20 eV and  ${\rm Be_2}^+$  at 50 eV must be attributed to physical sputtering. Auger neutralization of  ${\rm He}^+$  is still expected on theoretical grounds [31,32]. But it is difficult to be quantitative as to the efficiency. The similarities in the  ${\rm D}^+$  impact profiles for  ${\rm Be}^+$  and  ${\rm Be_2}^+$  with those for  ${\rm He}^+$  impact above approximately 50 eV suggests that physical sputtering is also occurring with  ${\rm D}^+$  at these impact energies (in the presence of some neutralization of  ${\rm D}^+$ ).

As regards the mechanism of Be dimer ion formation, we note that a previous molecular dynamics simulation of Cu dimer sputtering by  ${\rm Ar}^+$  suggests that direct ejection of intact dimers and recombination in or near the surface predominate, at least at 5 keV [34]. In our case,  ${\rm Be_2}^+$  formation could, in the first instance, be achieved by the higher energy impacting  ${\rm He}^+$  or  ${\rm D}^+$  ions (or He and D atoms) imparting enough energy to overcome the attractive interaction of a  ${\rm Be_2}^+$  dimer ion with its immediate Be metal environment. Alternatively, recombination of  ${\rm Be}^+$  with Be in or near the surface could be a source of  ${\rm Be_2}^+$ .

The sputtering profiles for  $BeO^+$  and  $Be_2O^+$ , which we ascribe to the presence of BeO and  $Be_2O$  impurities in the surface layer of Be, have minima at around 30 eV with  $D^+$  impact (see Fig. 6) and onsets at around 30 eV with  $He^+$  impact (see Fig. 5). We suggest mechanisms of formation of these ions similar to those suggested for the formation of  $Be^+$  and  $Be_2^+$ : chemically assisted with BeOD and  $Be_2OD$  as intermediates at low energies, and more direct physical sputtering (including recombination of  $Be^+$  with O to form  $BeO^+$  or with BeO to form  $Be_2O^+$ ) at high energies (above 30 eV) [35].

SDTrimSP 5.05 [36], a Monte-Carlo binary collision approximation (BCA) simulation with a Ziegler-Biersack-Littmark interaction potential and a 45° incident angle of projectiles relative to the surface was used to compare to the experimental data. In Fig. 8 the simulation data (open symbols) was added and scaled to fit the experimental data in arbitrary units at high collision energies. In the case of pure physical sputtering by helium projectiles, the general behaviour fits to the experimental data but the threshold energy is off by approximately 10 eV. Similar

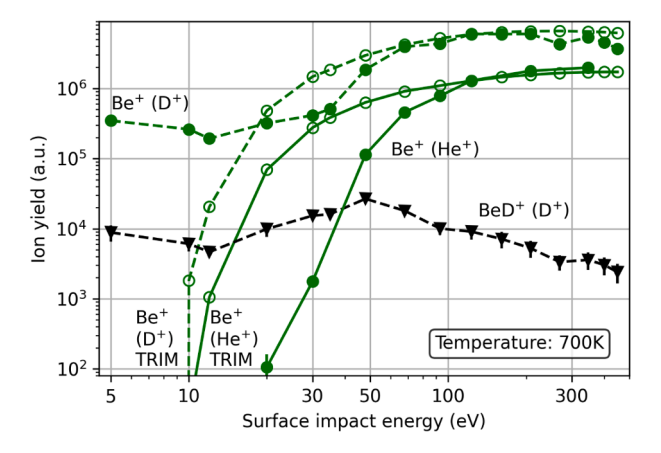


**Fig. 8.** Comparison of experimental data (solid symbols) with values obtained from a simulation (SDTrimSP 5.05, open symbols). Simulated data is scaled to fit experimental data at high surface impact energies.

deviations between BCA results and experiments were seen for light elements and low impact energies in the past [22]. For the deuterium projectiles, the experimental data do not show a threshold energy as seen in the SDTrimSP simulation. Considering that SDTrimSP uses pure atomic level BCA calculations this is no surprise but underlies the importance of chemical assisted sputtering which can be the dominant sputtering mechanism at low impact energies.

Production of BeH<sup>+</sup> and BeOH<sup>+</sup>: the influence of surface adsorbed water

Our previous measurements with  $D_2^+$  as the projectile provided evidence for BeH $^+$  formation from a surface reaction with adsorbed water; the production of both BeH $^+$  and BeOH $^+$  was observed to exhibit a clear dependence on the amount of water vapor introduced into the sample chamber [28]. Fig. 9 provides the profiles of sputtered BeH $^+$  and BeOH $^+$  measured in our D $^+$  and He $^+$  experiments that also can be attributed to adsorbed water on the Be sample: surface Be $^+$  can break the H-OH bond to form either BeH $^+$  or BeOH $^+$ . BeH $^+$  dominates over BeOH $^+$  at all impact energies in the D $^+$  experiments and above 50 eV in the He $^+$  experiments; both "track" the parent Be $^+$  profiles.

Fig. 10 shows the dependence of the relative ion yields of BeOH $^+$ /Be $^+$  and BeH $^+$ /Be $^+$  on the H $_2$ O pressure that we obtained (similar results were obtained with D $_2$ O). Argon ions with an impact energy of 208 eV were chosen as projectiles onto the Be surface heated to 480 K. An increase in the water pressure again leads to an increase in the relative

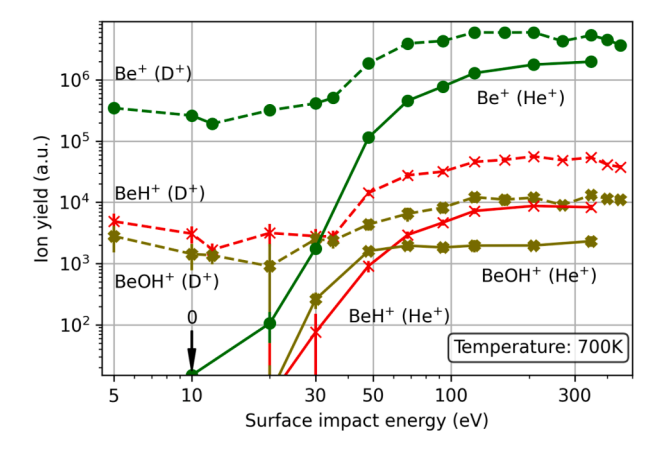


**Fig. 9.** Product ion yields in response to the surface impact energy (laboratory-frame) of  $D^+$  and  $He^+$  at a surface temperature of 700 K. ( $D^+$ ) yields are normalized to the projectile  $D^+$  ion current. The data point indicated with an arrow is below the noise level.

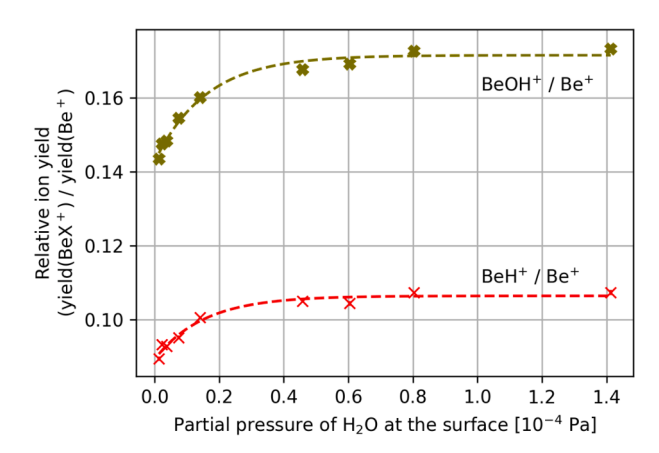


**Fig. 10.** Observed variation in the relative ion yields for  $BeOH^+/Be^+$  and  $BeH^+/Be^+$  with increasing pressure of  $H_2O$  for the impact of  $Ar^+$  projectile ions at 208 eV onto a beryllium surface heated to 480 K.

 $BeH^+$  yield which again is explained by the water molecules building a mono-layer of adsorbate on the Be surface [28]. The relative yield saturates once the formation of the monolayer is complete; the loss of water contact with the Be surface diminishes the formation of BeH $^+$  at lower partial pressures of  $H_2O$ . Similar results were obtained with  $He^+$  projectile ions in three experiments performed at different partial pressures of  $H_2O$  at impact energies of 347 and 68 eV where  $BeH^+$  dominates over  $BeOH^+$  (see Fig. 9).

#### Beryllium erosion

Our measurements indicate that the sputtered ions are dominated by atomic  $Be^+$  ions; molecular ions,  $BeX^+$ , have at least one order of magnitude lower yields than the  $Be^+$  yield which is comparable to the yield of impurity ions such as  $K^+$ .

Since neutrals are expected to be the dominant fraction of sputtered material and cannot be detected by our apparatus SurfTOF, a separate apparatus was recently constructed in our group to determine absolute sputtering yields with a quartz crystal microbalance, in a manner similar to that described by Smith and Ruzic [37,38]. In this apparatus an electron impact source ionizes  $D_2$  with 150 eV, the ions impinge the Be surface with an energy of 100 to 250 eV and a flux in the order of  $10^{19}\,$  m $^{-2}s^{-2}$ . Furthermore, the charge fraction of the sputtered beam could be estimated by replacing the quartz crystal microbalance with a Faraday cup. Preliminary results with this combined approach provide an estimate of the sputtered Be $^0$  neutral yield (actually Be $^0$  neutral + ion) of approximately 5% and an upper limit to the charged fraction of the sputtered beryllium of approximately 2%. Details about these measurements are provided in the supplementary material.

# Conclusions

We have successfully employed our "SurfTOF" tandem mass spectrometer apparatus to demonstrate the occurrence of physical and chemically assisted sputtering in a comparative study of He<sup>+</sup> and D<sup>+</sup> impact on a Be surface at projectile energies below 500 eV.

Both He<sup>+</sup> and D<sup>+</sup> ions were seen to physically erode Be predominantly as Be<sup>+</sup> and, above about 50 eV, also as trace amounts of Be<sub>2</sub><sup>+</sup>,  $\ll$  1%. Chemically assisted sputtering appears to be favored at lower energies, < 50 eV, of course only with D<sup>+</sup> projectiles.

In  $D^+$  sputtering,  $BeD^+$  is the signature ion for the occurrence of chemically assisted sputtering, because neutrals are not detectable with the SurfTOF setup. With the neutralization of impacting  $D^+$  by electron transfer from the surface metal, BeD becomes the preferred intermediate in the ultimate sputtering of  $Be^+$ .  $BeD_2^+$  [14] has not been observed.

These results imply that erosion of Be, in its use as the first wall for

the ITER blanket in fusion technology, caused by plasma  $D^+$ , and by inference  $T^+$ , is dominated by the sputtering of  $Be^+$ , and at least 10 times more by high energy impact ions, above 50 eV. The formation of  $D_2$  (or  $T_2$ ), would accompany the ultimate  $Be^+$  ion erosion via a BeD or BeT intermediate. The sputtering of dimer ions  $Be_2^+$  contributes only in a minor way.

In comparison, our results at energies below 50 eV show a preference of chemical sputtering and thus are relevant for ITER since it points to erosion on areas well separated from the core plasma.

The TOF spectra show that impurities in the Be, such as BeO, and background adsorbed molecules, such as  $H_2O$ , also can contribute to the erosion of Be by derivative ion sputtering with energetic plasma deuterons and deuterium radicals, and  $T^+$  and T radicals by implication, but these also would contribute only in a minor way.

Preliminary results of a combined approach with a quartz crystal microbalance and a Faraday cup provide absolute yields for sputtered beryllium neutrals and ions and an upper limit to the charged fraction of the sputtered beryllium of approximately 2%. The plasma sheath in fusion devices prevents low-energy ions sputtered from the walls from entering the plasma. However, chemical binding of tritium to beryllium in the wall contributes to tritium retention and the erosion of the wall itself are severe issues in fusion devices that use beryllium as a first wall material. Especially at low energies ignoring chemical assisted physical sputtering could lead to an underestimation of the total sputtering yield.

#### CRediT authorship contribution statement

Felix Duensing: Software, Writing – original draft. Faro Hechenberger: Investigation. Lorenz Ballauf: Conceptualization, Investigation. Anna Maria Reider: Investigation. Alexander Menzel: Resources. Fabio Zappa: Investigation, Writing – original draft. Timo Dittmar: Resources. Diethard K. Böhme: Writing – original draft. Paul Scheier: Writing – original draft, Project administration, Funding acquisition.

#### **Declaration of Competing Interest**

The authors declare that they have no known competing financial interests or personal relationships that could have appeared to influence the work reported in this paper.

# Acknowledgements

This work has been carried out within the framework of the EURO-fusion Consortium and has received funding from the Euratom Research and Training Programme 2014–2018 and 2019–2020 under grant agreement no. 633053. The views and opinions expressed herein do not necessarily reflect those of the European Commission. FD gratefully acknowledges support by the Friedrich Schiedel Foundation for Energy Technology "Reaktionen von Deuteriumionen an fusionsrelevanten Oberflächen". FH was supported by the Kernfusionsforschung KKKÖ – MG 2019-4.

# Appendix A. Supplementary data

Supplementary data to this article can be found online at https://doi.org/10.1016/j.nme.2021.101110.

#### References

- [1] J. Linke, J. Du, T. Loewenhoff, G. Pintsuk, B. Spilker, I. Steudel, M. Wirtz, Challenges for plasma-facing components in nuclear fusion, Matter. Radiat. Extremes 4 (5) (2019) 056201, https://doi.org/10.1063/1.5090100.
- [2] R.A. Pitts, S. Carpentier, F. Escourbiac, T. Hirai, V. Komarov, A.S. Kukushkin, S. Lisgo, A. Loarte, M. Merola, R. Mitteau, A.R. Raffray, M. Shimada, P.C. Stangeby, Physics basis and design of the ITER plasma-facing components, J. Nucl. Mater. 415 (1) (2011) S957–S964, https://doi.org/10.1016/j.jnucmat.2011.01.114.

- [3] E. Joffrin, S. Abduallev, M. Abhangi, et al., Overview of the JET preparation for deuterium-tritium operation with the ITER like-wall, Nucl Fusion 59 (11) (2019) 112021, https://doi.org/10.1088/1741-4326/ab2276.
- [4] J. Roth, E. Tsitrone, A. Loarte, T.h. Loarer, G. Counsell, R. Neu, V. Philipps, S. Brezinsek, M. Lehnen, P. Coad, C.h. Grisolia, K. Schmid, K. Krieger, A. Kallenbach, B. Lipschultz, R. Doerner, R. Causey, V. Alimov, W. Shu, O. Ogorodnikova, A. Kirschner, G. Federici, A. Kukushkin, Recent analysis of key plasma wall interactions issues for ITER, J. Nucl. Mater. 390-391 (2009) 1–9, https://doi.org/10.1016/j.inucmat.2009.01.037.
- [5] D.V. Andreev, V.N. Bespalov, A.J. Birjukov, B.A. Gurovich, P.A. Platonov, Postirradiation studies of beryllium reflector of fission reactor examination of gas release, swelling and structure of beryllium under annealing, J. Nucl. Mater. 233-237 (1996) 880–885, https://doi.org/10.1016/S0022-3115(96)00289-9.
- [6] M.G. Ganchenkova, V.A. Borodin, R.M. Nieminen, Hydrogen in beryllium: solubility, transport, and trapping, Phys. Rev. B 79 (13) (2009), 134101, https://doi.org/10.1103/PhysRevB.79.134101.
- [7] C.H. Skinner, A.A. Haasz, V.K. Alimov, N. Bekris, R.A. Causey, R.E.H. Clark, J. P. Coad, J.W. Davis, R.P. Doerner, M. Mayer, A. Pisarev, J. Roth, T. Tanabe, Recent advances on hydrogen retention in ITER's plasma-facing materials: beryllium, Carbon Tungsten Fus. Sci. Technol. 54 (4) (2008) 891–945.
- [8] A. Kirschner, K. Ohya, D. Borodin, R. Ding, D. Matveev, V. Philipps, U. Samm, Prediction of long-term tritium retention in the divertor of ITER: influence of modelling assumptions on retention rates, Phys. Scr. T138 (2009) 014011, https://doi.org/10.1088/0031-8949/2009/T138/014011.
- [9] S. Ueda, T. Ohsaka, S. Kuwajima, Molecular dynamics evaluation of self-sputtering of beryllium, J. Nucl. Mater. 258–263 (1998) 713–718, https://doi.org/10.1016/ S0022-3115(98)00251-7.
- [10] A. Kirschner, V. Philipps, J. Winter, U. Kögler, Simulation of the plasma-wall interaction in a tokamak with the Monte Carlo code ERO-TEXTOR, Nucl. Fusion 40 (5) (2000) 989–1001, https://doi.org/10.1088/0029-5515/40/5/311.
- [11] G. De Temmerman, R.P. Doerner, Deuterium retention and release in tungsten codeposited layers, J. Nucl. Mater. 389 (3) (2009) 479–483, https://doi.org/ 10.1016/j.inucmat.2009.03.028.
- [12] C. Björkas, K. Vörtler, K. Nordlund, D. Nishijima, R. Doerner, Chemical sputtering of Be due to D bombardment, New J. Phys. 11 (12) (2009) 123017, https://doi. org/10.1088/1367-2630/11/12/123017.
- [13] E. Safi, C. Björkas, A. Lasa, K. Nordlund, I. Sukuba, M. Probst, Atomistic simulations of the effect of reactor-relevant parameters on be sputtering, J. Nucl. Mater. 463 (2015) 805–809, https://doi.org/10.1016/j.jnucmat.2014.10.050.
- [14] A. Lasa, K. Heinola, K. Nordlund, The effect of beryllium on deuterium implantation in tungsten by atomistic simulations, Nucl. Fusion 54 (12) (2014) 123021, https://doi.org/10.1088/0029-5515/54/12/123021.
- [15] Q. Yu, M.J. Simmonds, R. Doerner, G.R. Tynan, L.i. Yang, B.D. Wirth, J. Marian, Understanding hydrogen retention in damaged tungsten using experimentallyguided models of complex multispecies evolution, Nucl. Fusion 60 (9) (2020) 096003. https://doi.org/10.1088/1741-4326/ab9b3c.
- [16] B. Wielunska, M. Mayer, T. Schwarz-Selinger, A.E. Sand, W. Jacob, Deuterium retention in tungsten irradiated by different ions, Nucl. Fusion 60 (9) (2020) 096002, https://doi.org/10.1088/1741-4326/ab9a65.
- [17] L. Chen, A. Kaiser, M. Probst, S. Shermukhamedov, Sputtering of the beryllium tungsten alloy Be<sub>2</sub>W by deuterium atoms: molecular dynamics simulations using machine learned forces, Nucl. Fusion 61 (1) (2021) 016031, https://doi.org/10.1088/1741-4326/abc9f4
- [18] A. Hakola, K. Heinola, K. Mizohata, J. Likonen, C. Lungu, C. Porosnicu, E. Alves, R. Mateus, I.B. Radovic, Z. Siketic, V. Nemanic, M. Kumar, C. Pardanaud, P. Roubin, Effect of composition and surface characteristics on fuel retention in beryllium-containing co-deposited layers, Phys. Scr. T171 (2020) 014038, https://doi.org/10.1088/1402-4896/ab4be8.
- [19] A. Mutzke, G. Bandelow, R. Schneider, Sputtering of mixed materials of beryllium and tungsten by hydrogen and helium, J. Nucl. Mater. 467 (2015) 413–417, https://doi.org/10.1016/j.jnucmat.2015.05.052.
- [20] R. Stadlmayr, P.S. Szabo, H. Biber, H.R. Koslowski, E. Kadletz, C. Cupak, R. A. Wilhelm, M. Schmid, C. Linsmeier, F. Aumayr, A high temperature dual-mode quartz crystal microbalance technique for erosion and thermal desorption spectroscopy measurements, Rev. Sci. Instrum. 91 (12) (2020) 125104, https://doi.org/10.1063/5.0012028.
- [21] J. Roth, E. Tsitrone, T. Loarer, V. Philipps, S. Brezinsek, A. Loarte, G.F. Counsell, R. P. Doerner, K. Schmid, O.V. Ogorodnikova, R.A. Causey, Tritium inventory in ITER plasma-facing materials and tritium removal procedures, Plasma Phys. Controlled Fusion 50 (10) (2008) 103001, https://doi.org/10.1088/0741-3335/50/10/103001
- [22] J. Roth, W. Eckstein, M. Guseva, Erosion of Be as plasma-facing material, Fusion Eng. Des. 37 (4) (1997) 465–480, https://doi.org/10.1016/S0920-3796(97)00091-
- [23] D. Nishijima, R.P. Doerner, M.J. Baldwin, G. De Temmerman, Erosion yields of deposited beryllium layers, J. Nucl. Mater. 390-391 (2009) 132–135, https://doi org/10.1016/j.jnucmat.2009.01.144.
- [24] J.N. Brooks, D.N. Ruzic, D.B. Hayden, Sputtering erosion of beryllium coated plasma facing components—general considerations and analysis for ITER detached plasma regime1Work supported by the Office of Fusion Energy, U.S. Department of Energy.1, Fusion Eng Des 37(4) (1997) 455-463. https://doi.org/10.1016/S0920-3796(97)00090-2.
- [25] C. Björkas, D. Borodin, A. Kirschner, R.K. Janev, D. Nishijima, R. Doerner, K. Nordlund, Molecules can be sputtered also from pure metals: sputtering of beryllium hydride by fusion plasma-wall interactions, Plasma Phys. Controll. Fusion 55 (7) (2013) 074004, https://doi.org/10.1088/0741-3335/55/7/074004.

- [26] S. Brezinsek, M.F. Stamp, D. Nishijima, D. Borodin, S. Devaux, K. Krieger, S. Marsen, M. O'Mullane, C. Bjoerkas, A. Kirschner, Study of physical and chemical assisted physical sputtering of beryllium in the JET ITER-like wall, Nucl. Fusion 54 (10) (2014) 103001, https://doi.org/10.1088/0029-5515/54/10/103001.
- [27] L. Ballauf, F. Duensing, F. Hechenberger, P. Scheier, A high sensitivity, high resolution tandem mass spectrometer to research low-energy, reactive ion–surface interactions, Rev. Sci. Instrum. 91 (6) (2020) 065101, https://doi.org/10.1063/ 1.5145170
- [28] L. Ballauf, F. Hechenberger, R. Stadlmayr, T. Dittmar, M. Daxner, S. Zöttl, F. Aumayr, Z. Herman, P. Scheier, Formation of beryllium-hydrogen ions in chemical sputtering from 20 to 420eV, Nucl. Mater. Energy 22 (2020) 100722, https://doi.org/10.1016/j.nme.2019.100722.
- [29] R. Chodura, in: Physics of plasma-wall interactions in controlled fusion, Springer US, Boston, MA, 1986, pp. 99–134, https://doi.org/10.1007/978-1-4757-0067-1\_4
- [30] H. Gabasch, F. Klauser, E. Bertel, T. Rauch, Coloring of topaz by coating and diffusion processes: an x-ray photoemission study of what happens beneath the surface, G&G 44 (2) (2008) 148–154.
- [31] H.D. Hagstrum, Theory of auger ejection of electrons from metals by ions, Phys. Rev. 96 (2) (1954) 336–365, https://doi.org/10.1103/PhysRev.96.336.

- [32] R. Souda, K. Yamamoto, W. Hayami, et al., Low-energy H+, He+, N+, O+, and Ne + scattering from metal and ionic-compound surfaces: neutralization and electronic excitation, Phys. Rev. B 51 (7) (1995) 4463, https://doi.org/10.1103/physrevb.51 4463
- [33] R. Souda, T. Aizawa, W. Hayami, et al., Neutralization of low-energy D+ scattered from solid surfaces, Phys. Rev. B 42 (13) (1990) 7761, https://doi.org/10.1103/ PhysRevB.42.7761.
- [34] M.H. Shapiro, T.A. Tombrello, A molecular dynamics study of Cu dimer sputtering mechanisms, Nucl. Instrum. Methods Phys. Res. Sect. B 84 (4) (1994) 453–464, https://doi.org/10.1016/0168-583X(94)95340-6.
- [35] E.A. Hodille, J. Byggmästar, E. Safi, K. Nordlund, Sputtering of beryllium oxide by deuterium at various temperatures simulated with molecular dynamics, Phys. Scr. T171 (2020) 014024, https://doi.org/10.1088/1402-4896/ab43fa.
- [36] A. Mutzke, R. Schneider, W. Eckstein, et al., SDTrimSP Version 5.00, Garching, 2011, p. 70. https://doi.org/11858/00-001M-0000-0026-EAF9-A.
- [37] P.C. Smith, D.N. Ruzic, Low energy (10 to 700 eV) angularly resolved sputtering yields for D+on beryllium, Nucl Fusion 38 (5) (1998) 673–680, https://doi.org/ 10.1088/0029-5515/38/5/303.
- [38] A.M. Reider, Ion-Surface Collisions on Beryllium: Absolute Rates of Physical Sputtering, M.Sc. thesis, University of Innsbruck, 2021.